# The application of a desiccant wheel to increase the energetic performances of a transcritical cycle

C. Aprea[1], A. Greco[2] *, A. Maiorino[1]

1 Dipartimento di Ingegneria Industriale, Università di Salerno, via Ponte Don Melillo, 84084 Fisciano, Salerno, Italia

2 DETEC, Università degli Studi di Napoli Federico II, P.le Tecchio 80, 80125 Napoli, Italia

* Corresponding author: Tel. +39 0817682289; Fax +39 0812390364; e-mail: adriana.greco@unina.it

Abstract

A desiccant dehumidification system with air can be driven by low grade (<80 °C) waste heat. In this paper, which is based on experimental data, the air flow at the outlet of the gas cooler of a trans-critical cycle is forced through a desiccant wheel regenerated by the air flow itself. The hybrid trans-critical refrigerator-desiccant system improves COP by approximately 77% as compared to a classical transcritical. The economical analysis suggests that the investment return-time is acceptable (lower than about 8 years) only at ambient temperature exceeding 35 °C. The ecological analysis indicates that the TEWI of the classical transcritical cycle exceeds that of the hybrid system, by approximately 60%.

Keywords

$CO_2$; Trans-critical cycle; Desiccant wheel; Hybrid system; Coefficient of Performance; Simple Pay Back Period; Discount Pay Back Period; TEWI.

## 1. Introduction

Over the last decades, the refrigeration, air conditioning and heat pump industry has been forced to undergo major changes, because of severe restrictions on refrigerant fluids.

The traditional refrigerants, i.e. ChloroFluoroCarbon (CFCs) and HydroChloroFluoroCarbon (HCFCs) fluids, were banned by the Montreal Protocol because of their contribution to the disruption of the stratospheric ozone layer. The HydroFluoroCarbon (HFCs) refrigerants that were expected to be acceptable permanent replacement are now on the list of regulated substances due to their impact on climate change. Indeed, according to the Kyoto Protocol, most HFCs have large Global Warming Potentials (GWPs) and, therefore provide a relevant, direct contribution to global warming when leaked to the atmosphere.

Considerable research effort was devoted to the development of environmentally-safe refrigeration systems, using natural working fluids. CO2, was considered as a promising alternative of HFCs. Indeed, Carbon dioxide is a component of the atmosphere, obtained from air itself by fractionation. Thus, it would have no impact on global warming, apart from for the energy consumption associated with the fractionation process.

$CO_2$ has many excellent advantages in engineering applications, such as no toxicity, no inflammability, higher volumetric capacity enabling compact systems, lower pressure ratio, better heat transfer properties, complete compatibility with normal lubricants, easy availability, lower price and no recycling problems [1], [2], [3]. The critical temperature of $CO_2$ (31.1 °C) is usually lower than typical heat rejection temperatures of air-conditioning and heat pump systems. This results in a trans-critical vapour compression cycle in lieu of a conventional one in water heating and comfort cooling and heating.

The performance of trans-critical $CO_2$ cooling system, however, is lower than that of conventional air-conditioners, due to large expansion losses and high irreversibility during the gas-cooling process [4]. Therefore, many researchers analyzed the performance of the trans-critical $CO_2$ refrigeration cycle, in order to identify opportunities to improve the energy efficiency of the system [5], [6], [7].

Among the improvement methods, many researchers analyzed the effect of an internal heat exchanger (IHX) to reduce throttling losses. Indeed, the discharge pressure that optimizes the COP is lower when the IHX is present. The data available in literature show a COP increase of around 10% [8], [9], [10], [11], [12], [13].

Further improvements to system performance in reducing expansion losses, are achieved by extracting and making use of the potentially available work, by means of an expander. Therefore, several authors analysed this possibility [14], [15], [16], [17], [18].

The performance deterioration of a basic, single-stage $CO_2$ cycle can be improved using a multi-stage compressor and inter-cooling of liquid and vapour refrigerant [19], [20], [21], [22], [23].

To improve the COP of the cycle, an ejector can be used in place of a throttling valve to recover some of the kinetic energy of the expansion process [24], [25], [26], [27], [28].

In this paper, a hybrid trans-critical refrigerator-desiccant wheel system was analyzed, in order to improve cycle performance.

Desiccant cooling consists in dehumidifying an air stream by forcing it through a desiccant material thus drying it to the desired indoor temperature. To afford continuous system performance, the adsorbed/absorbed vapour must be driven out the desiccant material (regeneration), so that it is dried enough to adsorbed water vapour in the next cycle [29], [30], [31], [32]. This process is carried out by heating the desiccant material to its regeneration temperature. The latter depends upon the nature of the desiccant used. For the last-generation desiccant materials, this temperature is within the range 50–75 °C, thus allowing the use of the air flow at the outlet of the gas cooler of the trans-critical cycle.

The study of the hybrid system discussed in this work is based on experimental data carried out with a prototype R744 system working as a classical split-system to cool air in a trans-critical cycle coupled with a desiccant cooling system.

## 2. The desiccant cooling

Desiccant cooling is based on air dehumidification by means of a desiccant substance (liquid or solid), and on its subsequent cooling. The desiccant cooling system consists in three main components: the regeneration heat source, the dehumidifier (desiccant material), and the cooling unit. The core of the system is the dehumidifier. Commonly used desiccant materials are: lithium chloride, triethylene glycol, silica gel, aluminium silicates, aluminium oxides, lithium bromide solution, etc. [33], [34]. Solid desiccant are compact, less subject to corrosion and carryover. A typical arrangement of a solid material is a slowly rotating wheel (6–30 revolutions/h) impregnated or coated with the desiccant, part of which intercepts the incoming air stream, while the rest is being regenerated.

The cooling unit can be the evaporator of a traditional air conditioner, an evaporative cooler or a cold coil. The regeneration heat source supplies the thermal energy necessary for driving out the moisture uptaken in the sorption phase. In this study is the hot air flow at the gas cooler outlet [35], [36], [37], [38].

The performance of a system based on desiccant cooling is represented by the psychometric chart in Fig. 1. The outdoor air stream at the state 1 is passed through rotary desiccant wheel. Its moisture is partly but significantly adsorbed by the desiccant material. The heat of adsorption elevates the temperature of the latter, so that a warm and quite dry air exits at state 2. The air stream is then cooled in a regenerative heat exchanger from the state 2 to state 3, and then in an evaporative cooler from state 3 to state 4. At this stage, the air is supplied to the air-conditioned volume.

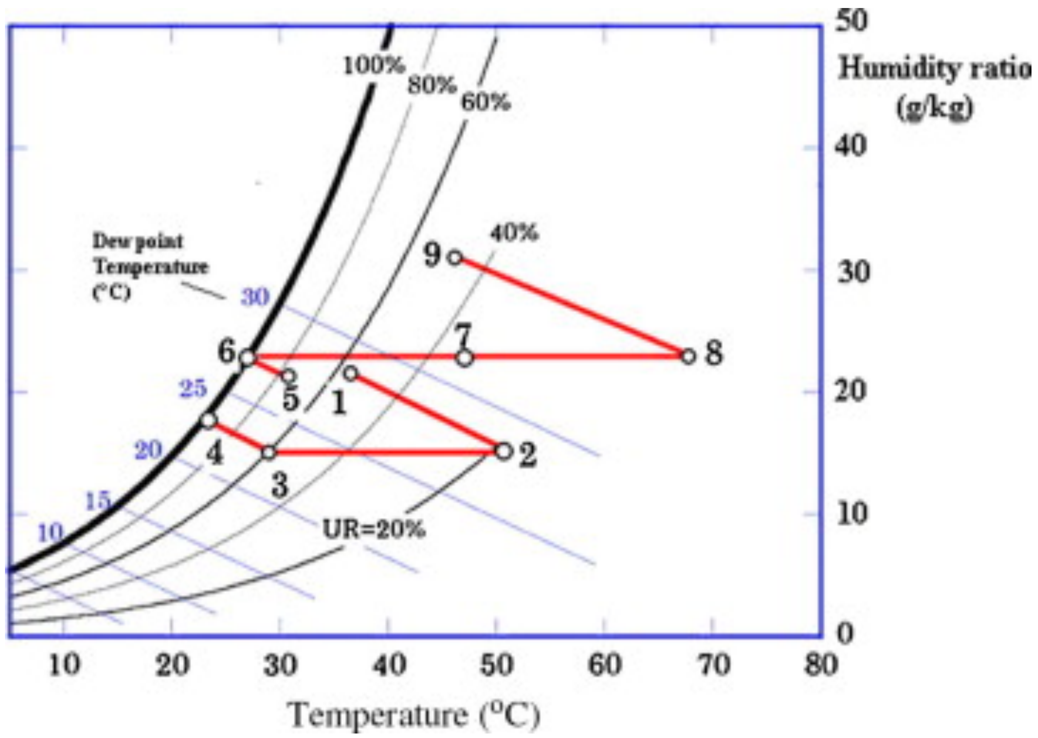

Fig. 1. Psychometric chart illustrating the transformations of a desiccant cooling system.

The air flow returned from latter is at the state 5. An evaporative cooler is used to cool down the return air from state 5 to state 6 and the cold air stream serves as heat sink to cool the supply air in the regenerative heat exchanger. Consequently, its temperature rises at the state 7. At this point, the air undergoes a complementary heating (7–8) to rich a high enough temperature as to enable the desiccant material regeneration (8–9). The regeneration heat can be supplied by free energy sources, e.g. by the air flow at the gas cooler exit .

## 3. The experimental transcritical cycle

Fig. 2 shows a sketch of the experimental transcritical cycle. Basically, there are two single-stage hermetic reciprocating compressors, an oil separator, an air gas-cooler, a liquid capacity, an air evaporator, an electronic expansion valve (EEV) and an electronically regulated back pressure valve (BPV) [39], [40], [41]. As regards the semi-hermetic main compressor, at an evaporation temperature of 5 °C and a gas-cooler exit temperature of 30 °C, at 80 bar, the refrigerating power is about 3000 W. An internal heat exchanger (IHX) is installed between the compressor suction and the exit of the gas-cooler. The lamination takes place by a back pressure valve and to the electronic expansion one. An auxiliary circuit by-passing the back-pressure valve is provide, in order to regulate the evaporation temperature. Some modulated electrical resistances, located in a thermally insulated channel where the air flows by means of a blower, enable the regulation of the temperature on the condenser and the simulation of external conditions.

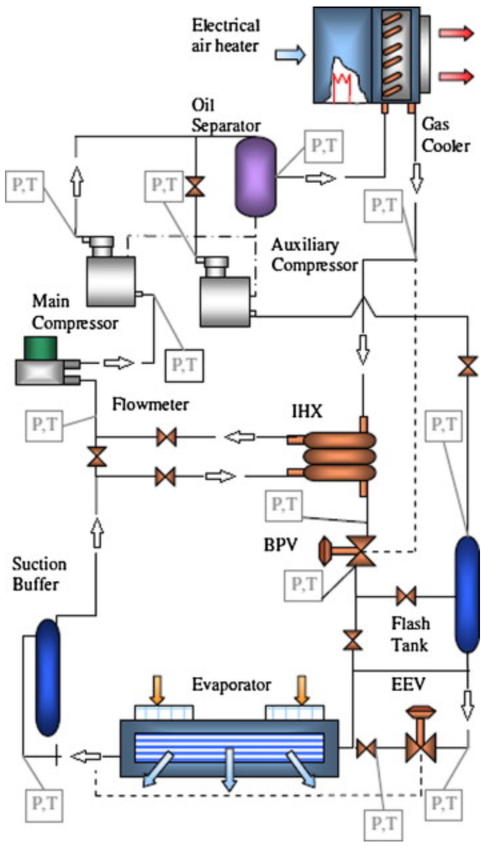


Fig. 2. A sketch of the transcritical cycle.

The plant is fully instrumented to evaluate the overall performances of the whole plant and those of each individual component. Carbon dioxide pressure and temperature are measured at the inlet and at the outlet of each device. The working fluid mass flow rate is monitored at the main compressor suction. Table 1 summarizes all the characteristics of the plant instrumentation.

Table 1. Transcritical cycle transducers specifications.

| Variable | Transducer | Uncertainty | Range |
|---|---|---|---|
| Temperature | Resistance thermometers Pt 100 | ±0.15 °C | −200–650 °C |
| Pressure | Piezoelectric | ±0.8% F.S. | 0–100 bar |
| Mass flow rate | Coriolis effect | ±0.2% | 0–100 g/s |
| Electric Power | Wattmeter | ±0.2% | 0.5–6 kW |

The Coefficient of Performance is evaluated as:

$$\mathrm{COP} = \frac{\dot{m}(h_{\mathrm{out,eV}} - h_{\mathrm{in,eV}})}{\dot{W}} = \frac{\dot{Q}_{\mathrm{eV}}}{\dot{W}} \tag{1}$$

4. The hybrid desiccant cooling-transcritical cycle

The setup for the desiccant cooling integrated with the transcritical cycle is shown schematically in Fig. 3. The return air incoming from the conditioned ambient flows through the evaporative cooling and then through the regenerative heat exchanger. At this point, it undergoes a complementary heating by the hot air flow at the gas cooler exit, in order to rich a sufficient temperature, as to regenerate the desiccant wheel [42].

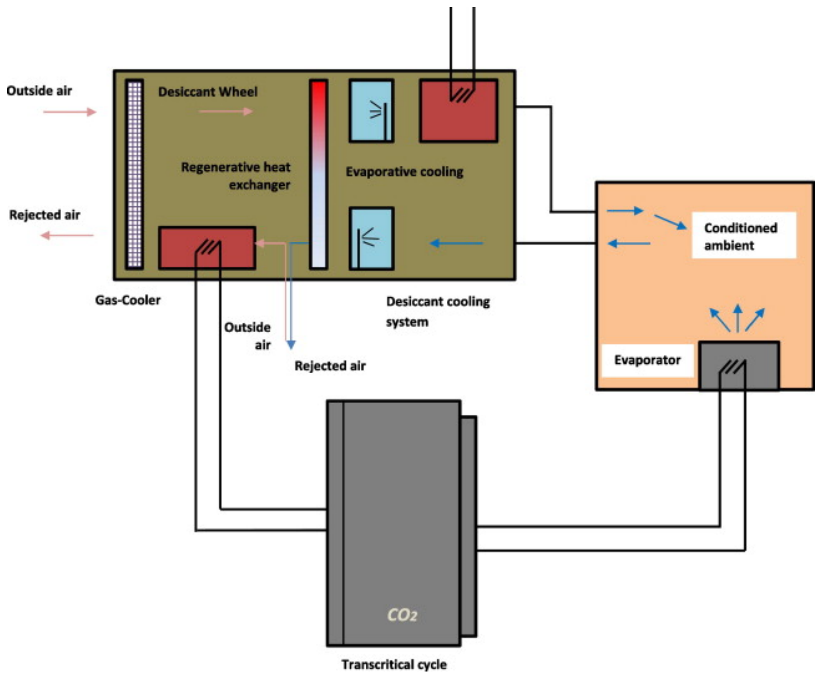


Fig. 3. A schematic of the hybrid desiccant cooling-transcritical cycle.

The outside air is dehumidified in the desiccant wheel. The heat of adsorption increases the air temperature. The air stream is subsequently cooled in the regenerative heat exchanger and then in the evaporative cooler. At this stage, the air is supplied to the ambient, upon cooling by the evaporator of the transcritical cycle.

The outside air volumetric flow rate of the experimental plant is 800 m3/h and the desiccant wheel used is the RC 0.6/1.5 (600 mm diameter). The desiccant material used in the desiccant wheel is silica gel. The external air temperature is evaluated with a resistance thermometer with an accuracy of ±0.15 °C. The air flow temperature and humidity measurements are carried out both at the inlet and at the outlet of the evaporator, at the inlet and at the outlet of the desiccant wheel and at the outlet of the desiccant cooling system. Air velocity is measured at the inlet of the evaporator channel and at the inlet of the desiccant wheel. The air velocity is measured with an Annubar Pitot device with an accuracy of ±1%; the air relative humidity is determined with a Peltier effect device with an accuracy of ±1%.

The Moisture Removal Capacity (MRC) of the desiccant wheel is defined as the mass flow rate of moisture removed by the wheel:

$$\mathrm{MRC} = \dot{V}_{\mathrm{air}}\,\rho_1(\omega_1 - \omega_2) \tag{2}$$

The Coefficient of Performance COPhyb of the hybrid desiccant cooling-transcritical cycle system is evaluated as:

$$\mathrm{COP}_{\mathrm{hyb}} = \frac{\dot{Q}_{\mathrm{eV}} + \dot{Q}_{\mathrm{a,d}}}{\dot{W} + \dot{Q}_{\mathrm{reg}}} \tag{3}$$

where   is the thermal power related to air dehumidification and is evaluated as (according to Fig. 1):

$$\dot{Q}_{\mathrm{air,d}} = \dot{m}_{\mathrm{air}}(h_5 - h_4) \tag{4}$$

$Q_{air,d}$ is the thermal power supplied for the regeneration process. In the hybrid system. this contribution is nil, since this power can be taken from the hot air flow at the gas cooler exit and therefore this contribution is equal to zero.

5. Experimental uncertainty

All tests are carried at steady-state conditions. Temperature and pressure values in key points of the plant were continuously monitored, in order to check the achievement of steady-state conditions.

Usually, the start up requires about 1 h for both plants. Steady state conditions are assumed to hold when the deviations of the controlled values from their corresponding mean values are lower than 0.5 °C for temperatures and 50 kPa for pressures. At this stage, the test started and the logging of data with 0.5 Hz acquisition frequency was performed on all channels for 60 s. For each channel, the 120 samples recorded were averaged. Each sample was checked against the corresponding mean value and it was rejected if it did not lay within the fixed range. If more than 5% of the samples were rejected, the whole test is discarded. Each test was iterated three times, in order to check reproducibility.

A personal computer connected with a data acquisition system, consisting of a controller, a channel scanner, and a multimeter was used to record the measurement data.

The data from the present study were classified as single sample. The uncertainty of each measured quantity consisted mainly of: uncertainty of the measurement device, uncertainty of the data-acquisition system, examination of system-sensor interaction errors, system disturbance errors.

A personal computer connected with a data acquisition system, consisting of a controller, a channel scanner, and a multimeter was used to record the measurement data.

In Table 2 uncertainties affecting each measured variable are estimated on the basis of the sensor error. The accuracy of all variables that are not accessible to direct measurement is estimated on the basis of error propagation method suggested by Moffat [43]. The data from the present study were classified as single sample. The uncertainty of each measured quantity consisted mainly of: uncertainty of the measurement device, uncertainty of the data-acquisition system, examination of system-sensor interaction errors, system disturbance errors.

Table 2. Uncertainties of experimental parameters.

| **Variable** | **Uncertainty (%)** |
|---|---|
| COP | ±3.8 |
| MRC | ±2.3 |
| $COP_{hyb}$ | ±4.4 |

6. Experimental results

Fig. 4 reports experimental MRC values, as a function of the regeneration air temperature. The measured volumetric air flow rate is 800 m3/h, with an inlet temperature of 32 °C and a relative humidity of 15 g/kg. The Fig. clearly shows that MRC increases with the regenerating air temperature.

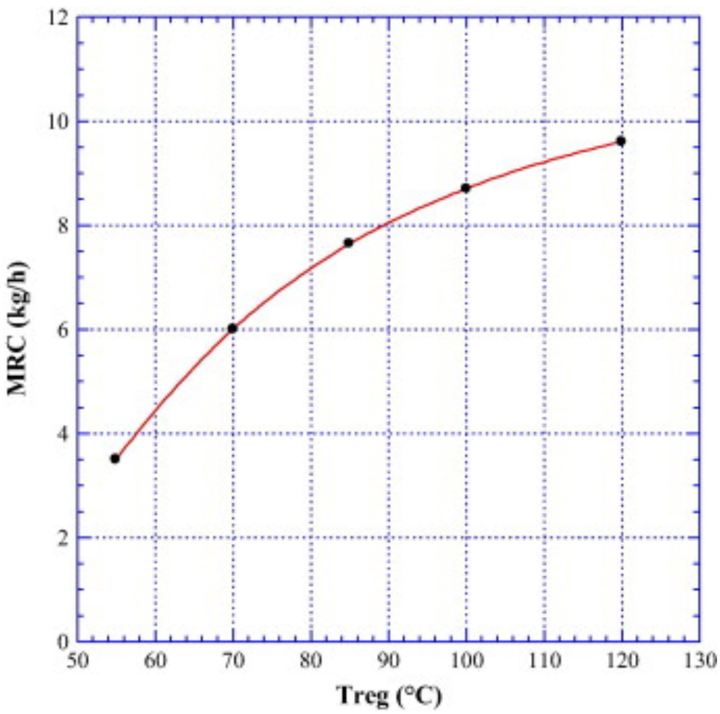


Fig. 4. MRC as a function of the regeneration air temperature, at V= 800 m3/h, Tair, inlet = 32 °C, ωair,inlet = 15 g/kg.

Three different sets of tests were carried out at different ambient temperatures (25, 30 and 35 °C, respectively) by modulating the electrical resistances at the inlet of the gas cooler air channel. All sets consist in five runs at different heat rejection pressure, as showed in Table 3.

Table 3. Experimental tests conditions.

| $T_{amb}$ (°C) | $P_{out,gc}$ (bar) | $\beta$ (–) |
|---|---|---|
| 25 | 80.3 | 2.2 |
| | 81.4 | 2.3 |
| | 84.7 | 2.4 |
| | 91.6 | 2.5 |
| | 93.0 | 2.6 |
| 30 | 86.9 | 2.2 |
| | 87.3 | 2.3 |
| | 90.5 | 2.4 |
| | 93.7 | 2.5 |
| | 98.1 | 2.6 |
| 35 | 89.2 | 2.3 |
| | 91.5 | 2.4 |
| | 96.2 | 2.5 |
| | 98.2 | 2.6 |
| | 101.0 | 2.7 |

In Fig. 5, Fig. 6, Fig. 7 the COP, the refrigerant power and the compression power of the transcritical cycle are been reported as a function of the compression ratio, at three different external temperature conditions. The figures clearly indicate that, by increasing the pressure at gas cooler outlet, both the compression and the refrigeration power increase with a different slope. The COP increases until the difference between change in slope of the refrigeration and of the compression power is positive, whereas the COP decreases as soon as the slope difference becomes negative. Therefore, for each ambient temperature, there is an optimal compression ratio that maximizes the COP.

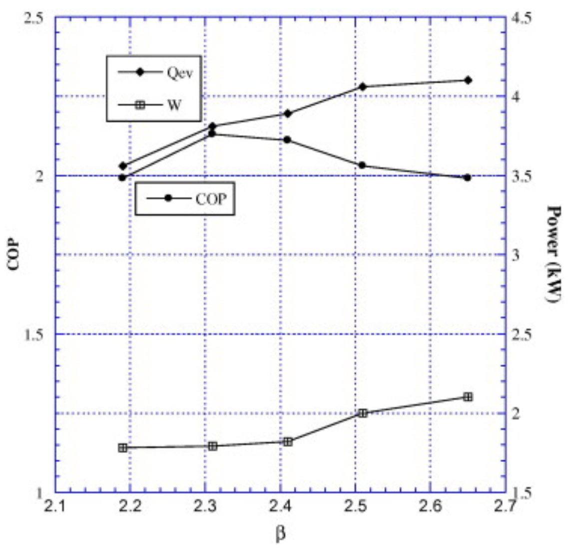

Fig. 5. COP, refrigerant power and compression power of the transcritical cycle as a function of the compression ratio at Tamb = 25 °C.

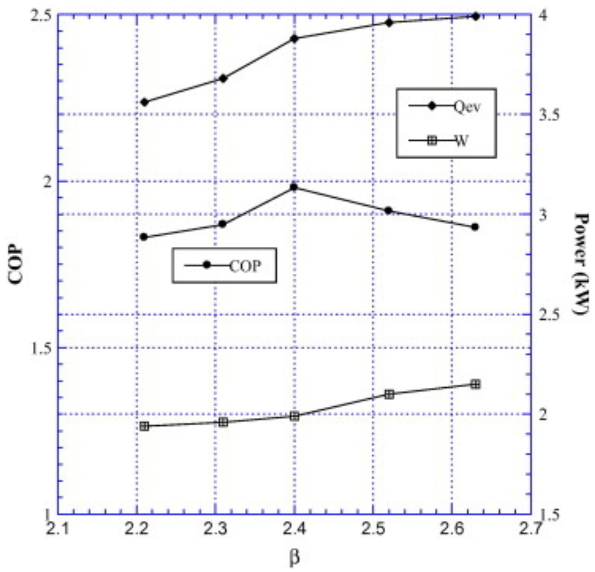


Fig. 6. COP, refrigerant power and compression power of the transcritical cycle as a function of the compression ratio at Tamb = 30 °C.

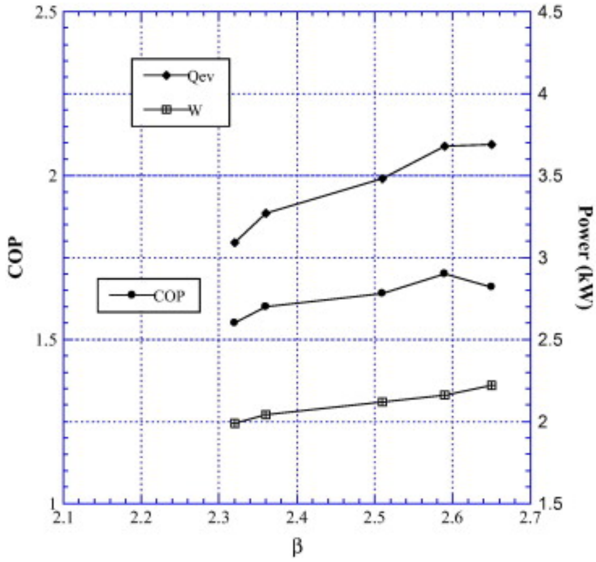


Fig. 7. COP, refrigerant power and compression power of the transcritical cycle as a function of the compression ratio at Tamb = 35 °C.

At any given compression ratio, the COP increases with decreasing ambient temperature. Indeed, with the decrease of the ambient temperature, the temperature of the CO2 at the gas cooler outlet decreases, as well. This leads to an increase in the enthalpy at the evaporator inlet and therefore to an increase of the refrigerant power at almost constant compression power.

In Fig. 8, COPhyb of the hybrid desiccant cooling-transcritical cycle system is reported, for the different ambient temperatures, as a function of the compression ratio. The figure clearly shows that, for each ambient temperature, there is a compression ratio that maximizing the performances of the hybrid system.

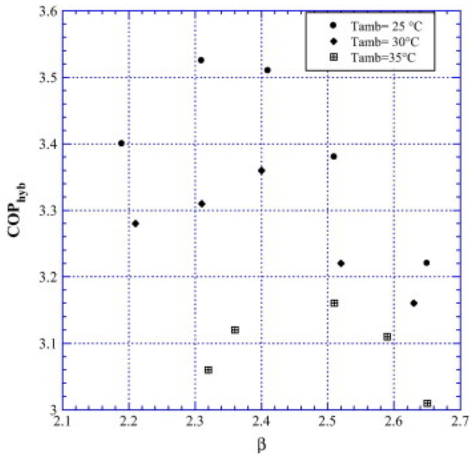


Fig. 8. COP the hybrid desiccant cooling-transcritical cycle systems as a function of the compression ratio at three different Tamb.

The COP of the hybrid system is greater than that of the simple transcritical system by a minimum of +62 to maximum of +97%, with a mean value of +77%. The maximum values correspond to the higher ambient temperature (i.e. 35 °C). Thus, increasing the ambient temperature increases the advantage in using the hybrid system, as well. Indeed, the Moisture Removal Capacity of the desiccant wheel increases with the regenerating air temperature together with the thermal power related to air dehumidification.

7. Economic analysis

Economic analysis of an investment is a prerequisite in order to determine the economic feasibility of the project.

In this analysis, the investment successfulness is evaluated in terms of investment return time, i.e. of Simple Pay Back Period:

$$\mathrm{SPB} = \frac{\Delta C}{\mathrm{ACI}} \tag{5}$$

where ΔC is the difference between cost of the traditional system and the proposed one; ACI is the annual energy cost savings of the proposed system.

One of the major disadvantages of simple payback period is that it ignores the time value of money. To counter this limitation, an alternative procedure called discounted payback period may be followed, which accounts for time value of money, by discounting the cash inflows of the project.

In Discounted Pay Back Period (DPB) the present value of each cash inflow has to be calculated taking the start of the first period as zero point. For this purpose, a suitable discount rate has to be set. The Discounted Cash Inflow for each period is to be calculated by the

$$\mathrm{DCI} = \frac{\text{Actual Cash Inflow}}{(1+i)^n} \tag{6}$$

where i is the discount rate, n is the period to which the cash inflow relates. The rest of the procedure is similar to the calculation of SPB except that we have to use the discounted cash flows, as calculated above, instead of actual cash flows. In this analysis, a 5% discount rate was assumed.

In the present analysis, a comparison between a simple transcritical cycle and a hybrid desiccant-transcritical system was carried out.

The costs of the desiccant cooling system are reported in Table 4. The cost of the hybrid system is the sum of the cost of the desiccant system and of the transcritical cycle. The cost of the traditional system is that of a transcritical cycle with a refrigerant load of $Q_{ev} + Q_{ad}$. The transcritical cycle is a prototype; the cost cannot be predetermined and therefore, in the present analysis, it is considered as a variable.

Table 4. Desiccant cooling system costs.

| Component | Cost (€) |
|---|---|
| Desiccant wheel | 3450 |
| Rotative heat exchanger | 450 |
| Air filter | 184.01 |
| Speed regulator air fan | 21.79 |
| Humidifier with electronic valve | 282.82 |
| Discharge air grid | 183.88 |
| Return air grid | 138.97 |
| Total | 4711.5 |

The annual electrical energy savings of the hybrid system depends on the price of electrical energy. Fig. 9 shows the yearly pattern of electricity price in Italy. The mean value of electrical energy in 2013 in Italy was 0.19035 €/kWh.

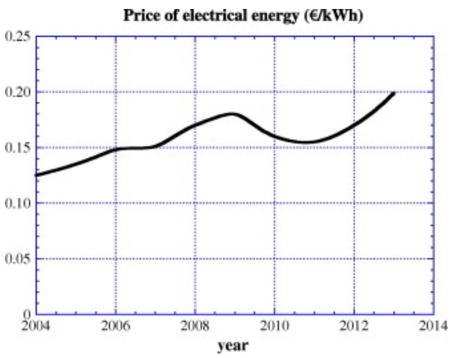

Fig. 9. Yearly pattern of electricity price in Italy.

The annual electrical energy with the hybrid system as a function of the compression ratio at the different ambient temperature is reported in Fig. 10. The figure clearly shows that, for each compression ratio, the annual saving is maximum at the maximum ambient temperature (i.e. 35 °C). Indeed, the Moisture Removal Capacity of the desiccant wheel increases with the regenerating air temperature. At fixed given external air temperature there is a compression ratio that maximizes the annual savings of the hybrid system.

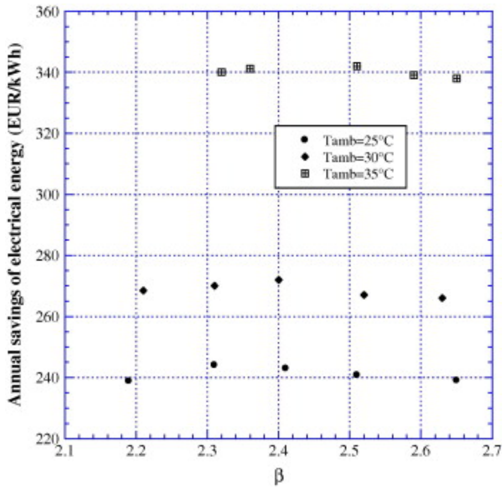


Fig. 10. Annual energy savings of the hybrid system as a function of the compression ratio at three different Tamb.

In Fig. 11, Fig. 12, Fig. 13 are reported SPB and DPB as a function of the transcritical cycle cost at 25, 30, and 35 °C ambient temperature, respectively. For each external ambient temperature, the indexes were evaluated for maximum, yearly, electrical energy savings. It is quite obvious that both SPB and DPB decrease with increasing transcritical cycle cost. The scenario with an external ambient temperature of 35 °C is the most favourable, since the investment return is lower.

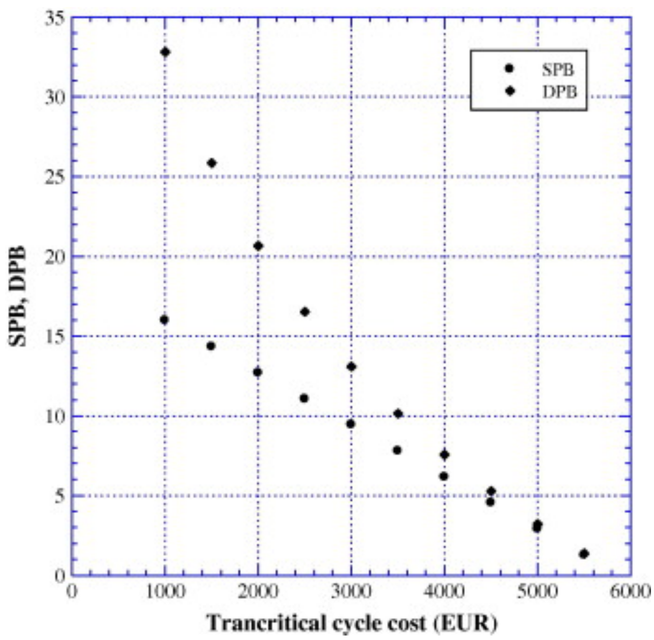


Fig. 11. SPB and DPB as a function of transcritical cycle cost at Tamb = 25 °C.

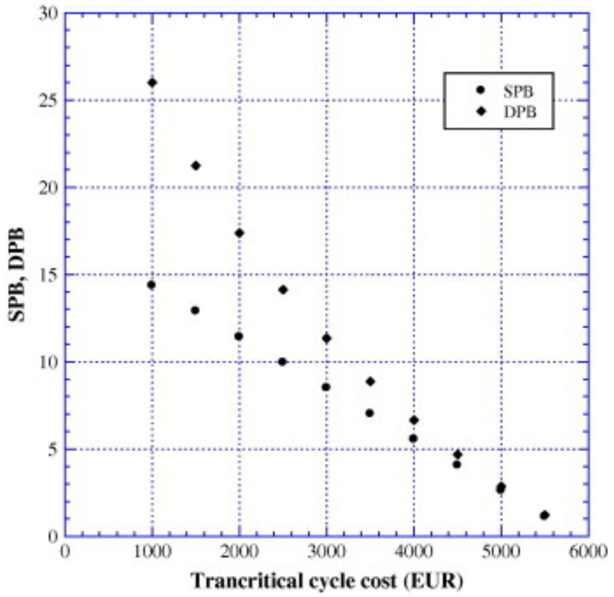


Fig. 12. SPB and DPB as a function of transcritical cycle cost at Tamb = 30 °C.

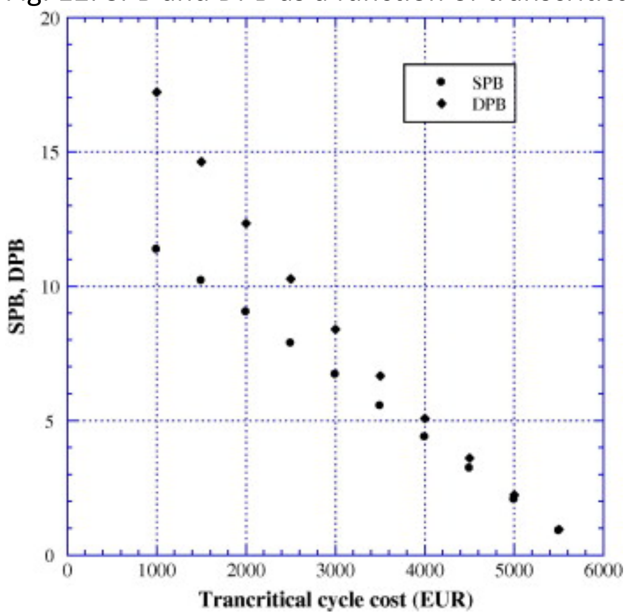


Fig. 13. SPB and DPB as a function of transcritical cycle cost at Tamb = 35 °C.

The reference cost for the transcritical cycle is that of a classical vapour compression plant working in the same operating conditions with R410A as a refrigerant fluid (Daikin); i.e. 3000 €. For a transcritical cycle cost exceeding 3000 €, SPB is lower than 9.4, 8.5, and 6.7, respectively, for an ambient temperature of 25, 30, and 35 °C; whereas DPB is less than 13, 11, and 8.4, respectively.

8. Ecological analysis

In this paragraph an ecological analysis of the hybrid system is afforded.

The effect of refrigerant plants on ambient are related to global warming. Vapour compression plants yield both a direct and an indirect contribution to global warming. The former depends on the GWP of refrigerant fluids and on the fraction of refrigerant charge released in the atmosphere during operation and maintenance, or which is not recovered when the system is scrapped. For $CO_2$ GWP is equal to 1 and, therefore, the direct effect is negligible as compared to the indirect one. The indirect contribution is energy-related. Indeed, a vapour compression refrigerator requires electrical energy produced by a power plant that typically burns a fossil fuel, thus releasing CO2 in the atmosphere. The amount of released CO2 is a strong function of the COP of the vapour compression plant, of the power plant efficiency and of the fuel used in the conversion plant that affect the emissions per unit energy converted. The typical power-plant technology adopted varies from one country to another. The literature provides some indicative, average levels of CO2 release per KWh of electrical energy for various countries. For Italy, the value is 0.59 kg CO2/kWhe.

TEWI is the sum of the direct contribution of the greenhouse gases used to make or operate the systems and the indirect contribution of carbon dioxide emissions resulting from the energy required to run the systems over their normal lifetimes [44].

The TEWI is calculated as:

$$\begin{aligned} &\mathrm{TEWI} = \mathrm{CO}_{2,\mathrm{dir}} + \mathrm{CO}_{2,\mathrm{indir}} \ (\mathrm{kg\ CO_2}) \\ &\mathrm{CO}_{2,\mathrm{dir}} = \mathrm{RC} \cdot p_{\mathrm{L}} \cdot V \cdot \mathrm{GWP} \quad (\mathrm{kg\ CO_2}) \\ &\mathrm{CO}_{2,\mathrm{indir}} = \alpha \cdot \frac{\dot{Q}_{\mathrm{ref}}}{\mathrm{COP}} \cdot H \cdot V \ (\mathrm{kg\ CO_2}) \end{aligned} \tag{7}$$

As already stated, the indirect contribution to TEWI consists in the so-called energy-related contribution [45], [46], [47].

Table 5 reports the parameters adopted for the TEWI evaluation.

Table 5. Parameters in TEWI evaluation.

| **Parameter** | **Value** |
|---|---|
| $H$ | 918 h |
| PL | 10% year |
| $V$ | 1 year |
| $\alpha$ | 0.59 kg $CO_2$/kWh$_e$ |

In Fig. 14, Fig. 15, Fig. 16 the TEWI of the hybrid system and that of the transcritical cycle are reported as a function of the compression ratio at 25, 30, and 35 °C external temperature, respectively. The figures clearly show that TEWI of the classical transcritical cycle is always higher than that of the hybrid system. The difference increases with ambient temperature and ranges between the +38 and +99%.

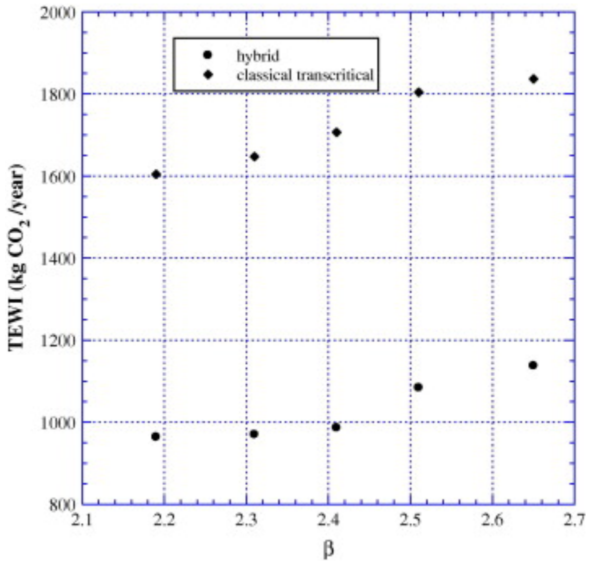

Fig. 14. TEWI of the transcritical cycle and of the hybrid system as a function of the compression ratio at Tamb = 25 °C.

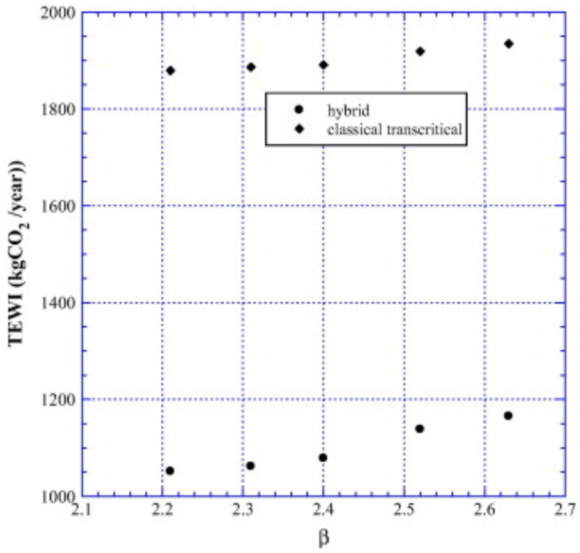

Fig. 15. TEWI of the transcritical cycle and of the hybrid system as a function of the compression ratio at Tamb = 30 °C.

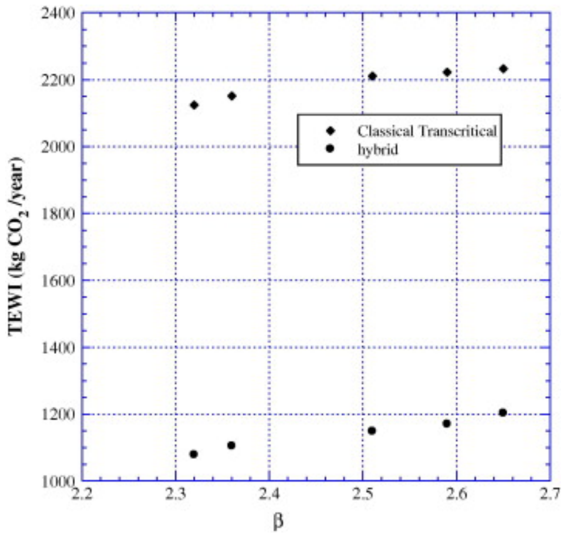

Fig. 16. TEWI of the transcritical cycle and of the hybrid system as a function of the compression ratio at Tamb = 35 °C.

## 9. Conclusions

$CO_2$, was considered as a promising alternative of HFCs. The critical temperature of CO2 (31.1 °C) is usually lower than typical heat rejection temperatures of air-conditioning and heat pump systems. This results in a trans-critical vapour compression cycle. The performance of a trans-critical CO2 cooling system, however, is lower than that of conventional air-conditioners, due to large expansion losses and high irreversibility during the gas-cooling process. In this paper a hybrid trans-critical refrigerator-desiccant wheel system was analyzed, in order to improve the cycle performances.

In this system, the air flow at the outlet of the gas cooler of the trans-critical cycle is used to bring the desiccant material up to its regeneration temperature. The study of the hybrid system is based on experimental data. The experimental tests discussed in this study are carried out with a prototype R744 system working as a classical split-system to cool air in a trans-critical cycle.

On the basis of an energetic, economic, ecological analyses the following conclusions can be drawn:

• The COP of the hybrid system is greater than that of the simple transcritical system by a minimum of +62 up to maximum of +97%, with a mean value of +77%. The maximum values correspond to the highest ambient temperature (i.e. 35 °C).

• The economic analysis shows that the scenario with an external ambient temperature of 35 °C is the most favourable, since the investment return time is lower than about 8 years.

• The ecological analysis indicates that the TEWI of a classical transcritical cycle is always higher than that of the hybrid system. The difference increases with the ambient temperature and ranges between the +38% and +99%.

## References

[1] Lorentzen G, Petterson J. A new efficient and environmentally benign system for air-conditioning. Int J Refrig 1993;16(1):4–12.

[2] Lorentzen G. Revival of carbon dioxide as a refrigerant. Int J Refrig 1994;17(5):292–301.

[3] Lorentzen G. The use of natural refrigerants: a complete solution to the CFC/ HCHC predicament. Int J Refrig 1995;18(3):190–7.

[4] Aprea C, Greco A, Maiorino A. The substitution of R134a with R744: an exergetic analysis based on experimental data. Int J Refrig 2013;36(8):2148–59. http://dx.doi.org/10.1016/j.ijrefrig.2013.06.012.

[5] Amir F, Ting DS, Yang WW. Second law analysis of the transcritical CO2 refrigeration cycle. Energy Convers Manage 2004;45(13–14):2269–81.

[6] Sarkar J, Bhattacharyya S, Ram Gopal M. Transcritical CO2 heat pump systems: exergy analysis including heat transfer and fluid flow effects. Energy Convers Manage 2005;46(13–14):2053–67.

[7] Peñarrocha I, Llopis R, Tárrega L, Sánchez D, Cabello R. A new approach to optimize the energy efficiency of CO2 transcritical refrigeration plants. Appl Therm Eng 2014;67(1–2):137–46.

[8] Sánchez D, Patiño J, Llopis R, Torrella E, Fuentes FV. New positions for an internal heat exchanger in a CO2 supercritical refrigeration plant. Experimental analysis and energetic evaluation. Appl Therm Eng 2014;63(1):129–39.

[9] Boewe D, Bullard C, Yin J, Hrnjak PS. Contribution of internal heat exchanger to transcritical R744 cycle performance. Int J HVAC&R Res 2001;7(2):155–68.
[10] Tao YB, Tao WQ, Wu ZG. Experimental study on the performance of CO2 residential air-conditioning system with an internal heat exchanger. Energy Convers Manage 2010;51(1):64–70.
[11] Chen Y, Gu JJ. The optimum high pressure for CO2 transcritical refrigeration systems with an internal heat exchangers. Int J Refrig 2005;28(8):1238–49.
[12] Aprea C, Maiorino A. An experimental evaluation of the transcritical CO2 refrigerator performances using an internal heat exchanger. Int J Refrig 2008;31:1006–11.
[13] Tao YB, He YL, Tao WQ, Wu ZG. Experimental study on the performance of CO2 residential air-conditioning system with an internal heat exchanger. Energy Convers Manage 2010;51(4):64–70.
[14] Robinson D, Groll E. Efficiencies of transcritical CO2 cycle with and without an expansion turbine. Int J Refrig 1998;21(7):577–89.
[15] Ma Y, Wei D, Za S, Li M. Thermodynamic analysis and compression expander for CO2 transcritical cycle. In: The fifth IIR-Gustav Lorentzen conference on natural working fluids, Guangzhou, China; 2002: p. 292–7.
[16] Baek JS, EGroll A, Lawless PB. Piston cylinder work producing expansion device in a carbon dioxide cycle. Part I: experimental investigation. Int J Refrig 2005;28:141–51.
[17] Baek JS, Groll EA, Lawless PB. Piston cylinder work producing expansion device in a carbon dioxide cycle. Part I: theoretical investigation. Int J Refrig 2005;28:152–64.
[18] Tian Hua, Ma Yitai, Li Minxia, Wang Wei. Study on expansion power recovery in CO2 trans-critical cycle. Energy Convers Manage 2010;51(12):2516–22.
[19] Inagaki M, Sasaya H, Osakli Y. Pointing to the future: two stage CO2 compression, heat transfer issues in natural refrigerants. Int Inst Refrig 1997;24:131–40.
[20] Hogli W, Yitai M, Jingrui T, Minxia L. Theoretical analysis and experimental research on transcritical CO2 two stage compression cycle with two gas coolers (TSCC + TG) and the cycle with intercooler (TSCC + IC). Energy Convers Manage 2011;25(89):2819–28.
[21] Kim SG, Kim MS. Experiment and simulation on the performance of an autocascade refrigeration system using carbon dioxide as a refrigerant. Int J Refrig 2002;25:1093–101.
[22] Groll EA, Baek S, Lawless PB. Effect of pressure ratio across compressors on the performance of the transcritical CO2 cycle with two-stage compression and intercooling. In: The international refrigeration and air conditioning conference, Purdue; 2002: p. R11–7.
[23] Eskandari Nanjili F, Yavari MA. Performance of a new two-stage multi intercooling transcritical CO2 ejector refrigeration cycle. Appl Therm Eng 2012;40:202–9.
[24] Liu JP, Chen JP, Chen ZJ. Thermodynamic analysis on the transcritical R744 vapor-compression/ejection hybrid refrigeration cycle. In: The fifth IIR-Gustav Lorentzen conference on natural working fluids, Guangzhou, China; 2002: p. 184–8.
[25] Pianthong K, Seehanam W, Behnia M, Sriveerakul T, Aphornratana S. Investigation and improvement of ejector refrigeration system using computational fluid dynamics technique. Energy Convers Manage 2007;48(9):2556–64.
[26] Yu J, Ren Y, Chen H, Li Y. Applying mechanical subcooling to ejector refrigeration cycle for improving the coefficient of performance. Energy Convers Manage 2007;48(4):1193–9.
[27] Li Xinguo, Huang Haijun, Zhao Wenjing. A supercritical or transcritical Rankine cycle with ejector using low-grade heat. Energy Convers Manage 2014;78:551–8.
[28] Habibzadeh A, Rashidi MM, Galanis N. Analysis of a combined power and ejector-refrigeration cycle using low temperature heat. Energy Convers Manage 2013;65:381–91.
[29] Lazzarin RM, Gasparella A. New ideas for energy utilisation in combined heat and power with cooling: I. Principles. Appl Therm Eng 1997;17(4):369–84.

[30] Lazzarin RM, Gasparella A. New ideas for energy utilisation in combined heat and power with cooling: II. Applications. Appl Therm Eng
1997;17(4):479–500.
[31] Daou K, Wang RZ, Xia ZZ. Desiccant cooling air conditioning: a review. Renew Sustain Energy Rev 2006;10:55–77.
[32] Uçkan Irfan, Yılmaz Tuncay, Hürdog_ ˘an Ertaç, Büyükalaca Orhan. Experimental investigation of a novel configuration of desiccant based evaporative air conditioning system. Energy Convers Manage 2013;65:606–15.
[33] Cortés Farid B, Chejne Farid, Carrasco-Marín Francisco, Pérez-Cadenas Agustín F, Moreno-Castilla Carlos. Water sorption on silica-and zeolite-supported hygroscopic salts for cooling system applications. Energy Convers Manage 2012;53(1):219–23.
[34] Zhang XJ, Qiu LM. Moisture transport and adsorption on silica gel–calcium chloride composite adsorbents. Energy Convers Manage 2007;48(1):320–6.
[35] Zhang LZ, Niu JL. Performance comparisons of desiccant wheels for air dehumidification and enthalpy recovery. Appl Therm Eng 2002;22:1347–67.
[36] Ghali K. Energy savings potential of a hybrid desiccant dehumidification air conditioning system in Beirut. Energy Convers Manage 2008;49(11):3387–90.
[37] Angrisani G, Capozzoli A, Minichiello F, Roselli C, Sasso M. Desiccant wheel regenerated by thermal energy from a microcogenerator: experimental assessment of the performances. Appl Energy 2011;88:1354–65.
[38] Angrisani G, Minichiello F, Roselli C, Sasso M. Experimental analysis on the dehumidification and thermal performance of a desiccant wheel. Appl Energy 2012;92:563–72. performances, Applied Energy 88, p.1354–1365.
[39] Aprea C, Maiorino A. Transcritical CO2 refrigerator and sub-critical R134a refrigerator: a comparison of the experimental results. Int J Energy Res 2009;33:1040–7.
[40] Aprea C, Maiorino A. Heat rejection pressure optimization for a carbon dioxide split system: an experimental study. Appl Energy 2009;861:2373–80.
[41] Aprea C, Greco A, Maiorino A. An experimental study on charge optimization of a trans-critical CO2 cycle. Int J Environ Sci Technol 2013. http://dx.doi.org/ 10.1007/s13762-014-0502-6.
[42] La Dong, Li Yong, Dai Yanjun, Ge Tianshu, Wang Ruzhu. Effect of irreversible processes on the thermodynamic performance of open-cycle desiccant cooling cycles. Energy Convers Manage 2013;67:44–56.
[43] Moffat RJ. Using uncertainty analysis in the planning of an experiment. Trans ASME J Fluids Eng 1985;107:173–8.
[44] Aprea C, Greco A. An experimental evaluation of the greenhouse effect in R22 substitution. Energy Convers Manage 1998;39(9):877–87.
[45] Aprea C, Greco A, Maiorino A. An experimental evaluation of the greenhouse effect in the substitution of R134a with CO2. Energy 2012;45:753–61.
[46] Aprea C, Greco A, Maiorino A. Global warming impact of substitution of traditional refrigerant fluids in vapour compression plants: an experimental study, In: Global Warming. ISBN 979-953-307-820-4, Ed. InTech.; 2012.
[47] Aprea C, Greco A, Maiorino A. An experimental evaluation of the greenhouse effect in the substitution of R134a with CO2. Energy 2012;45:753–61.